Available online at www.sciencedirect.com

SciVerse ScienceDirect

Procedia Computer Science 9 (2012) 1129 – 1138

Procedia Computer Science

International Conference on Computational Science, ICCS 2012

Polynomial Chaos Quadrature-based minimum variance approach for source parameters estimation

R. Madankan[a], P. Singla[a,1,*], A. Patra[a], M. Bursik[b], J. Dehn[e], M. Jones[c], M. Pavolonis[f], B. Pitman[d], T. Singh[a], P. Webley[e]

[a]*Department of Mechanical & Aerospace Engineering, University at Buffalo*
[b]*Department of Geology, University at Buffalo*
[c]*Center for Computational Research, University at Buffalo*
[d]*Department of Mathematics, University at Buffalo*
[e]*Geophysical Institute, University of Alaska, Fairbanks*
[f]*NOAA-NESDIS, Center for Satellite Applications and Research*

Abstract

We present a polynomial chaos based minimum variance formulation to solve inverse problems. The utility of the proposed approach is evaluated by considering the ash transport problem arising due to volcanic eruption. Volcanic ash advisory centers generally makes use of mathematical models for column eruption and advection and diffusion of ash cloud in atmosphere. These models require input data on source conditions such as vent radius, vent velocity and distribution of ash-particle size. The inputs are usually not well constrained, and estimates of the uncertainty in the inputs is needed to make accurate predictions of cloud motion. The recent eruption of Eyjafjallajökull, Iceland in April 2010 is considered as test example. For validation, the `puff` advection and diffusion model is used to hindcast the motion of the ash cloud through time concentrating on the period 14-16 April 2010. Variability in the height and loading of the eruption is introduced through the volcano column model `bent`. Output uncertainty due to uncertain input parameters is determined with a polynomial chaos quadrature (PCQ)-based sampling of the multidimensional puff input vector space. Furthermore, the posterior distribution for input parameters is obtained by assimilating satellite imagery data with PCQ predictions using a minimum variance approach.

Keywords: inverse problem, source parameter estimation, polynomial chaos, minimum variance estimator

1. Introduction

Across the world, ash clouds are produced by explosive eruptions from volcanoes. These clouds are a serious hazard to aircraft, causing damage to the engines [1]. More recently, the eruption at Eyjafjallajökull, Iceland, has wreaked havoc on European aviation after the eruption started on April 14, 2010. In this case, the closure of European air-space resulted in more than $4 billion in economical losses and with more than 10 million stranded passengers[2]. With the growing fear of natural, accidental or deliberate release of toxic agents, there is tremendous interest in

*Email address: psingla@buffalo.edu (P. Singla)
[1]Corresponding author

1877-0509 © 2012 Published by Elsevier Ltd.
doi:10.1016/j.procs.2012.04.122

generating accurate hazard maps of toxic material dispersion and multi-hypothesis forecasting for appropriate disaster management.

Volcanic Ash Advisory Centers (VAAC) routinely use both satellite data and numerical modeling to assist in their planning for hazard response and mitigation. At present, examination of satellite data provides the best quantitative method for detecting and analyzing ash clouds. However, satellite imagery data is limited in terms of the kind and frequency of observations that can be taken and may only provide access to limited aspects of the dispersion of ash cloud. For example, satellite images can only tell where the ash was. To predict the position and motion of ash clouds, advection/dispersion models are solved numerically. For example, during the Eyjafjallajökulleruption, the London VAAC used the NAME computational model [3] of ash advection and dispersion to make predictions of the likely position of the ash cloud and issue advisories to the airline industry. Other VAACs use different but similar computational models. These models may incorporate stochastic variability, such as a varying windfield that transports ash particles. In addition, these models often require input data on source conditions such as eruption plume height that is not well characterized. These factors cause overall accuracy to degrade as the model output evolve. The fusion of observational (satellite) data with numerical simulation promises to provide greater understanding of physical phenomenon than either approach alone can achieve. In other words, the optimal solution should be a weighted mixture of model forecast and observation data.

Both the ENSEMBLE platform (http://ensemble2.jrc.ec.europa.eu/) and the Harmonisation initiative (http://harmo.org) point to the importance of ensemble forecasting in numerical weather prediction and dispersion modeling. Work under both ENSEMBLE and Harmonisation umbrellas has laid out many of the principles and pathways to ensemble forecasting, and progress has been made on presenting the results of tens of model runs in a coherent fashion [4]. Nevertheless, rigorous sampling strategies that can be implemented in a reasonable time, and quantitative estimation of central tendency in outputs together with error estimates, are still lacking. the main objective of this contribution is to provide accurate estimates for volcano source parameters along with associated statistical bounds. This approach had its birth with the development of the Kalman Filter [5].

Kalman Filter (KF) is the optimal Bayesian estimator for linear systems with initial condition and measurement errors assumed to be Gaussian. However, the performance of the Kalman filter can deteriorate appreciably due to model parameter uncertainty [6, 7]. The sensitivity of the KF to parametric modeling errors has led to the development of several robust filtering approaches; robust in the sense that they attempt to limit, in certain ways, the effect of parameter uncertainties on the overall filter performance. Alternatively, when the model parameters are uncertain, the estimation is carried out through the simultaneous estimation of states and parameters (also viewed as states), which results in a nonlinear filtering problem even for otherwise linear systems [8]. Methods like the extended Kalman Filter (EKF) [6] or Unscented Kalman Filter (UKF) [9] have been used to estimate model parameters along with state estimates. Although both the EKF and UKF based filters are very popular for simultaneous state and parameter estimation problems, both methods are based upon very restrictive Gaussian error assumption for both parameter and state uncertainty. Clearly, the Gaussian assumption can work well for moderately nonlinear systems but it might not be appropriate at all for certain problems based upon the physical model. For example, Gaussian distribution is not an ideal distribution to represent errors in the eruption column height which is a positive quantity. This necessitates the need for filters which can incorporate the knowledge about non-Gaussian uncertainty. Various researches have endeavored to exploit knowledge of statistics, dynamic systems and numerical analysis to develop nonlinear filtering techniques [10–13] which cater to the various classes of state and parameter estimation problems. For low-order nonlinear systems, the Particle Filter (PF) [12, 13] has been gaining increasing attention. However, Daum in his seminal work[14] discusses that various factors like *volume of state space in which conditional pdf is non-vanishing, rate of decay of the conditional pdf in state space, stationarity of the problem, effective dimensionality of the problem, etc.* strongly affect the computational complexity and performance of the particle filter [14].

Recently, the polynomial chaos (PC) based estimation algorithms have garnered attention for parameter estimation problem. The main principle of the PC approach is to expand random variables using polynomial basis functions that are orthogonal with respect to the pdf of the parameters (Hermite polynomials for normally distributed parameters, Legendre for uniformly distribution, etc.), and transform stochastic equations into deterministic equations in higher dimensional projection space using Galerkin collocation. The polynomial chaos has been used in different ways for parameter estimation problem also popular in literature as *inverse problem*. The PC approach has been successfully used in conjunction with the Ensemble Kalman Filter (EnKF) for input parameter estimation [15]. Pence *et al.* [16] have used the PC formulation to obtain maximum likelihood estimates for input parameters while Blanchard *et al.*

[17] have used the PC formulation in a Bayesian framework to provide the a-posteriori estimates. In Refs. [18], the PC based minimum variance estimator have been developed to provide estimates for posterior moments of both parameters and system states. The main advantage of this approach is that it provides point estimates for both the state and parameters along with statistical confidence bounds associated with these estimates described in terms of the posterior moments. In this paper, we will utilize this minimum variance estimator to estimate posterior density function for volcano source parameters.

2. Volcanic Plume Models

Particle transport models can be divided into two broad categories: those intended to calculate eruption column characteristics based on tephra fall deposits, as in [19], and those intended to predict long-range atmospheric and deposit distributions based on the scale of the eruption, as in [20]. Both types of models rely on the existence of an explicit relationship between the eruption and atmospheric dynamics and the resulting fall deposit. This relationship is complicated by a number of factors, including plume mechanics, variable weather conditions, and particle re-entrainment. Our interest is in the movement of ash clouds, and not in tephra deposition. Therefore, we focus attention on long-range modeling and consider a simple particle transport model, but one that nonetheless contains several sources of uncertainty.

Tanaka [21] and Searcy et al. [22] developed `puff`, an ash tracking model for predicting the paths of young volcanic clouds. `puff` simplifies the eruption plume to a vertical source, and uses a Lagrangian pseudo-particle representation of the ash cloud in a detailed 3-D regional windfield to determine the trajectory of the cloud. `puff` and other dispersion models have proven extremely useful in modeling the distal transport of ash for aviation safety [22]. During an eruption crisis, `puff` predictions have been used to estimate ash cloud movement critical to the assessment of potential impacts – for example, on aircraft flight paths. `puff` has been validated against historic volcanic eruptions such as the 1992 Crater Peak vent eruption at Mount Spurr and the 2006 eruption at Mount Augustine with reasonable success [22, 23].

To initialize a `puff` simulation a collection of particles of different sizes must be specified as a function of altitude. This distribution is often inferred from historical eruption and plume observations, and is not well constrained; see [24–26]. It is important to remember that `puff` particles are not simple surrogates for ash concentration, but are representatives of ejecta of a given size at some initial height. As such this number is a user-selected input, and affects the simulation time and resolution of the output. In addition to particle distribution and windfield, other `puff` input parameters include the coefficients of turbulent diffusion and particle fallout, both of which are estimated.

Instead of guessing the initial particle distribution as a function of height, we employ a volcanic eruption plume model called `bent` to provide initial conditions; the essential features of this coupling are described in [26]. `bent` solves a cross-sectionally averaged system of equations for continuity, momentum and energy balance [24–26], as a function of the eruption vent radius and speed of the ejecta. `bent` assumes a distribution of pyroclasts of different sizes, and the model equations then predict the height distribution of the various sized clasts. `bent` has been tested against plume rise height data, and against dispersal data [24]; the discussion in that paper corroborates that the scaling relationships derived in [27] between energy and plume rise height are valid for energetic volcanic plumes piercing the tropopause.

Using `bent` to provide initial conditions for `puff` incorporates important plume physics into our cloud transport simulations. On the one hand, physics guides our model coupling and largely determines for us how outputs from `bent` feed into `puff`. On the other hand, this coupling can be thought of as substituting one set of uncertain parameters (vent size, velocity, clast size distribution) for an uncertain function (initial particle height distribution). In this way, inputs from the source, together with their variability, can be modeled and propagated through `bent` and `puff`. A detailed sensitivity analysis could relate the variations in input parameters to characteristics of the cloud as output, but this result is itself somehat incomplete. Instead we employ uncertainty analysis, which casts a much broader net in terms of assessing confidence of predictions based on all available information.

3. Methodology

In the standard `puff` model, one tracks the position of representative particles as they are transported by wind and turbulence, and the position of each parcel is assumed to be a deterministic quantity. Instead of solving for the point

position of the puff particles, we consider the particles representing a probability distribution. That is, the position of a particle is assumed to be a random variable, $\mathbf{x}_k$, whose time evolution is given by a stochastic differential equation, which should be thought of as generalizing the puff advection/diffusion equation, written generically as:

$$\dot{\mathbf{x}} = \mathbf{f}(t, \mathbf{x}, \boldsymbol{\Theta}) \tag{1}$$

In Eq. (1), $\boldsymbol{\Theta}$ represents uncertain volcano source parameters such as the vent radius, vent velocity, mean grain size and grain size variance. The total uncertainty associated with the state vector $\mathbf{x}_k = \mathbf{x}(t_k)$ is characterized by the probability distribution function (pdf) $p(t_k, \mathbf{x}_k)$. The index k denotes the discrete time-step in the evolution of p. That is, we replace the time evolution of the state vector $\mathbf{x}_k$ by the time evolution of the pdf $p(t_k, \mathbf{x}_k)$.

Several approximate techniques exist in the literature to approximate the state pdf evolution, the most popular being Monte Carlo (MC) methods [28], Gaussian closure [29], and Equivalent Linearization [30]. All of these algorithms except MC methods are similar in several respects, and are suitable only for linear or moderately nonlinear systems, because the effect of higher order terms can lead to significant errors. Monte Carlo methods require extensive computational resources and effort, and become increasingly infeasible for high-dimensional dynamic systems [14]. The next section discusses the Polynomial Chaos Quadrature (PCQ) method for solving the time evolution of state pdf for systems that include initial condition and parametric uncertainty.

3.1. Polynomial Chaos Quadrature

The propagation of uncertainty due to time-invariant but uncertain input parameters can be approximated by a generalization of polynomial chaos [31]. Generalized PC is an extension of the homogenous chaos idea of [32] and involves a separation of random variables from deterministic ones in the solution algorithm for a stochastic differential equation. The random variables are expanded in a polynomial expansion. Suitably chosen polynomials converge rapidly to the assumed pdf for the input variables.

$$\dot{\mathbf{x}}(t, \boldsymbol{\Theta}) = \mathbf{f}(t, \boldsymbol{\Theta}, \mathbf{x}), \quad \mathbf{x}(t_0) = \mathbf{x}_0 \tag{2}$$

where $\mathbf{u}(t)$ is the input of dynamic system at time t, $\mathbf{x}(t, \boldsymbol{\Theta}) = [x_1(t, \boldsymbol{\Theta}), x_2(t, \boldsymbol{\Theta}), \cdots, x_n(t, \boldsymbol{\Theta})]^T \in \mathbb{R}^n$ represents the stochastic system state vector, and uncertain parameter vector $\boldsymbol{\Theta} = [\boldsymbol{\Theta}_1, \boldsymbol{\Theta}_2, \cdots, \boldsymbol{\Theta}_m]^T \in \mathbb{R}^m$ is assumed to be time invariant and function of a random vector $\boldsymbol{\xi} = [\xi_1, \xi_2, \cdots, \xi_m]^T \in \mathbb{R}^m$ defined by a pdf $p(\boldsymbol{\xi})$ over the support Ω. Please note that $\mathbf{f}(t, \boldsymbol{\Theta}, \mathbf{x})$ can be a nonlinear function in general. The PC expansion for the state vector $\mathbf{x}$ and uncertain parameter $\boldsymbol{\Theta}$ can be written as:

$$x_i(t, \boldsymbol{\Theta}) = \sum_{k=0}^{N} x_{i_k}(t)\phi_k(\boldsymbol{\xi}) = \mathbf{x}_i^T(t)\boldsymbol{\Phi}(\boldsymbol{\xi}) \Rightarrow \mathbf{x}(t, \boldsymbol{\xi}) = \mathbf{X}_{pc}(t)\Phi(\boldsymbol{\xi}) \tag{3}$$

$$\theta_i(\boldsymbol{\xi}) = \sum_{k=0}^{N} \theta_{i_k}\phi_k(\boldsymbol{\xi}) = \boldsymbol{\Theta}_i^T\boldsymbol{\Phi}(\boldsymbol{\xi}) \Rightarrow \boldsymbol{\Theta}(t, \boldsymbol{\xi}) = \boldsymbol{\Theta}_{pc}\Phi(\boldsymbol{\xi}) \tag{4}$$

where, $\mathbf{X}_{pc}$ and $\boldsymbol{\Theta}_{pc}$ are matrices composed of coefficients of PC expansion for state $\mathbf{x}$ and parameter $\boldsymbol{\Theta}$, respectively. Similar to the linear case, coefficients θ_{i_k} are obtained by making use of following *normal equations*:

$$\theta_{i_k} = \frac{\langle \theta_i(\boldsymbol{\xi}), \phi_k(\boldsymbol{\xi}) \rangle}{\langle \phi_k(\boldsymbol{\xi}), \phi_k(\boldsymbol{\xi}) \rangle} \tag{5}$$

Now, substitution of Eq. (3) and Eq. (4) into Eq. (2), leads to:

$$\mathbf{e}_i(\mathbf{X}_{pc}, \boldsymbol{\xi}) = \sum_{k=0}^{N} \dot{x}_{i_k}(t)\phi_k(\boldsymbol{\xi}) - \mathbf{f}_i(t, \mathbf{X}_{pc}(t)\Phi(\boldsymbol{\xi}), \boldsymbol{\Theta}_{pc}\Phi(\boldsymbol{\xi})), \quad i = 1, 2, \cdots, n \tag{6}$$

$n(N+1)$ time-varying coefficients x_{i_k} can be obtained using the Galerkin process, i.e. projecting the error captured in Eq. (6) onto space of basis functions $\phi_k(\boldsymbol{\xi})$. For polynomial or rational state nonlinearity, the Galerkin process will lead to a set of $n(N+1)$ *nonlinear deterministic differential equations*. For non-polynomial nonlinearity such

as transcendental or exponential functions, difficulties may arise during the computation of projection integrals. To manage the non-polynomial nonlinearity difficulties in polynomial chaos integration, Dalbey *et al.* have proposed a formulation [33] known as Polynomial Chaos Quadrature (PCQ). PCQ replaces the projection step of the PC with numerical quadrature. The resulting method can be viewed as a MC-like evaluation of system equations, but with sample points selected by quadrature rules. To illustrate this, consider Eq. (2), which by substitution of Eq. (3) and Eq. (4) can be written as:

$$\sum_{k=0}^{N} \dot{x}_{i_k}(t)\phi_k(\boldsymbol{\xi}) - \mathbf{f}_i(t, \mathbf{X}_{pc}(t)\Phi(\boldsymbol{\xi}), \boldsymbol{\Theta}_{pc}\Phi(\boldsymbol{\xi})) = 0, \quad i = 1, \cdots, n \tag{7}$$

The projection step of PC yields:

$$\sum_{k=0}^{N} \langle \phi_k(\boldsymbol{\xi}), \phi_j(\boldsymbol{\xi}) \rangle \dot{x}_{i_k} - \langle \mathbf{f}_i(t, \mathbf{X}_{pc}(t)\Phi(\boldsymbol{\xi}), \boldsymbol{\Theta}_{pc}\Phi(\boldsymbol{\xi})), \phi_j(\boldsymbol{\xi}) \rangle = 0 \quad i = 1, \cdots, n, \quad j = 0, \cdots, N \tag{8}$$

In the case which $f(t, \mathbf{x}, \boldsymbol{\Theta})$ is linear, it is possible to evaluate projection integrals of Eq. (8) analytically. More generally, the starting point of PCQ methodology is to replace the exact integration with respect to $\boldsymbol{\xi}$ by numerical integration. The familiar Gauss quadrature method is a suitable choice for most cases. This yields:

$$\langle \phi_i(\boldsymbol{\xi}), \phi_j(\boldsymbol{\xi}) \rangle = \int \phi_i(\boldsymbol{\xi})\phi_j(\boldsymbol{\xi})p(\boldsymbol{\xi})d\boldsymbol{\xi} \simeq \sum_{q=1}^{M} w_q \phi_i(\boldsymbol{\xi}_q)\phi_j(\boldsymbol{\xi}_q) \tag{9}$$

$$\langle \mathbf{f}_i(.), \phi_j(\boldsymbol{\xi}) \rangle = \int \mathbf{f}_i(t, \mathbf{X}_{pc}(t)\Phi(\boldsymbol{\xi}), \boldsymbol{\Theta}_{pc}\Phi(\boldsymbol{\xi}))\phi_j(\boldsymbol{\xi})p(\boldsymbol{\xi})d\boldsymbol{\xi} \simeq \sum_{q=1}^{M} w_q \mathbf{f}_i(t, \mathbf{X}_{pc}(t)\Phi(\boldsymbol{\xi}_q), \boldsymbol{\Theta}_{pc}\Phi(\boldsymbol{\xi}_q))\phi_j(\boldsymbol{\xi}_q) \tag{10}$$

where M is the number of quadrature points used. Substitution of aforementioned approximation of stochastic integral in Eq. (8) and interchanging summation and differentiation leads to

$$\frac{d}{dt} \sum_{q=1}^{M} \sum_{k=0}^{N} w_q \phi_j(\boldsymbol{\xi}_q)\phi_k(\boldsymbol{\xi}_q)x_{i_k} - \sum_{q=1}^{M} w_q \mathbf{f}_i(t, \mathbf{X}_{pc}(t)\Phi(\boldsymbol{\xi}_q), \boldsymbol{\Theta}_{pc}\Phi(\boldsymbol{\xi}_q))\phi_j(\boldsymbol{\xi}_q) = 0 \tag{11}$$

which can be simplified as:

$$\frac{d}{dt} \sum_{q=1}^{M} \phi_j(\boldsymbol{\xi}_q)x_i(t, \boldsymbol{\xi}_q)w_q - \sum_{q=1}^{M} w_q \mathbf{f}_i(t, \mathbf{X}_{pc}(t)\Phi(\boldsymbol{\xi}_q), \boldsymbol{\Theta}_{pc}\Phi(\boldsymbol{\xi}_q))\phi_j(\boldsymbol{\xi}_q) = 0 \tag{12}$$

Integrating with respect to time t yields:

$$\sum_{q=1}^{M} (x_i(t, \boldsymbol{\xi}_q) - x_i(t_0, \boldsymbol{\xi}_q))\phi_j(\boldsymbol{\xi}_q)w_q - \int_{t_0}^{t} \sum_{q=1}^{M} w_q \mathbf{f}_i(t, \mathbf{X}_{pc}(t)\Phi(\boldsymbol{\xi}_q), \boldsymbol{\Theta}_{pc}\Phi(\boldsymbol{\xi}_q))\phi_j(\boldsymbol{\xi}_q)dt = 0 \tag{13}$$

Interchanging the order of time integration and quadrature summation leads to

$$\sum_{q=1}^{M} \left\{ x_i(t, \boldsymbol{\xi}_q) - x_i(t_0, \boldsymbol{\xi}_q) - \int_{t_0}^{t} \mathbf{f}_i(t, \mathbf{X}_{pc}(t)\Phi(\boldsymbol{\xi}_q), \boldsymbol{\Theta}_{pc}\Phi(\boldsymbol{\xi}_q))dt \right\} \phi_j(\boldsymbol{\xi}_q)w_q = 0 \quad i = 1, \cdots, n \tag{14}$$

Note that the integral expression in Eq. (14) can be evaluated by an integration of the model equation with a specific instance of the random variable $\boldsymbol{\xi}_q$. Thus the process of evaluating the statistics on the output of the system reduces to sampling the chosen input points guided by quadrature method. Finally, the coefficients of the PC expansion can be obtained as:

$$x_{i_k}(t) = \frac{1}{d_k^2} \sum_{q=1}^{M} \mathcal{X}_i(t_0, t, \boldsymbol{\xi}_q)\phi_k(\boldsymbol{\xi}_q)w_q, \quad k, j = 0, 1, \cdots, N, \;\; i = 1, 2, \cdots, n \tag{15}$$

where

$$\mathcal{X}_i(t_0, t, \boldsymbol{\xi}_q) = x_i(t_0, \boldsymbol{\xi}_q) + \int_{t_0}^{t} \mathbf{f}_i(t, \mathbf{X}_{pc}(t)\Phi(\boldsymbol{\xi}_q), \boldsymbol{\Theta}_{pc}\Phi(\boldsymbol{\xi}_q)),\ d_k^2 = \int_{\Omega} \phi_k(\boldsymbol{\xi})\phi_k(\boldsymbol{\xi}) p(\boldsymbol{\xi}) d\boldsymbol{\xi} \tag{16}$$

Hence, the resulting method can be viewed as a MC-like evaluation of system equations, but with sample points selected by quadrature rules. PCQ approximates the moment of system state as:

$$\mathbf{E}[x_i(t)^N] = \int_{\Omega} \left(\int_{t_0}^{t} \dot{x}_i dt \right)^N dp(\boldsymbol{\xi}) = \int_{\Omega} \left(x_i(t_0, \boldsymbol{\xi}) + \int_{t_0}^{t} \mathbf{f}_i(t, \mathbf{x}, \boldsymbol{\Theta}) dt \right)^N dp(\boldsymbol{\xi}) \quad i = 1, 2, \cdots, n \tag{17}$$

$$= \sum_q w_q \left[\mathcal{X}_i(t_0, t, \boldsymbol{\xi}_q) \right]^N \quad i = 1, 2, \cdots, n \tag{18}$$

In other words, the output moments are approximated as a weighted sum of the output of simulations run at carefully selected values of the uncertain input parameters (namely the quadrature points). The classic method of Gaussian quadrature exactly integrates polynomials up to degree $2N + 1$ with $N + 1$ quadrature points. The tensor product of 1–dimensional quadrature points is used to generate quadrature points in general n-dimension parameter space. As a consequence, the number of quadrature points increases as $(N + 1)^n$ to integrate exactly an n-variate polynomial of degree $2N + 1$ as the number of input parameters increases.

PCQ can still suffer from underintegration error if an insufficient number of samples is used. This necessitates an adaptive or nested quadrature scheme to successively refine the accuracy by increasing the number of sample points. In a nested quadrature scheme, one can compare the solution computed at a given order with that of a quadrature rule of lower order, which evaluates the integrand at a subset of the original N points, to minimize the integrand evaluations. Gaussian quadrature rules are not naturally nested. Hence, we employ Clenshaw–Curtis quadrature [34, 35] for numerical integration. The Clenshaw–Curtis scheme is based on an expansion of the integrand in terms of Chebyshev polynomials and naturally leads to nested quadrature rules. Another advantage of Clenshaw–Curtis quadrature is that the quadrature weights can be evaluated in order $N\log N$ time by fast Fourier transform algorithms as compared to order N^2 for the Gaussian quadrature weights.

4. Fusion of Measurement Data and Process Model

In the previous section, the PCQ approach is discussed in detail as a tool to propagate the state and parameter uncertainty through a VATD model coupled with column eruption model. The use of sensor data to correct and refine the dynamical model forecast so as to reduce the associated uncertainty is a logical improvement over purely model-based prediction. However, mathematical models for various sensors are generally based upon the "usefulness" rather than the "truth" and do not provide all the information that one would like to know. Care must be taken when assimilating the observational data. In this section, PCQ based minimum variance approach has been developed to integrate multiple sources of complementary information with system dynamics to help reduce the uncertainty of the output. The proposed approach make use of the PCQ methodology to evaluate the high fidelity prediction between two measurement intervals and updates the PC series expansion based upon minimum variance formulation.

Using the PCQ uncertainty evolution as a forecasting tool , the joint state and parameter pdf can be updated using the Bayes' rule on the arrival of a measurement data:

$$p(\boldsymbol{\Theta}, \mathbf{x}|\mathbf{Y}_k) = \frac{p(\boldsymbol{\Theta}, \mathbf{x}|\mathbf{Y}_{k-1}) p(\mathbf{y}(t_k)|\boldsymbol{\Theta}, \mathbf{x})}{p(\mathbf{y}(t_k))} \tag{19}$$

where $\mathbf{Y}_k$ represents the measurement data up to time t_k. $p(\boldsymbol{\Theta}, \mathbf{x}|\mathbf{Y}_{k-1})$ is the joint prior pdf (solution of the PCQ approach) of $\mathbf{x}$ and $\boldsymbol{\Theta}$ at time t_k given all observations up to time t_{k-1}, $p(\mathbf{y}_k|\boldsymbol{\Theta}, \mathbf{x})$ is the likelihood that we observe $\mathbf{y}_k$ given $\mathbf{x}$ and $\boldsymbol{\Theta}$ at time t_k and $p(\boldsymbol{\Theta}, \mathbf{x}|\mathbf{Y}_k)$ represents the joint posterior pdf of $\mathbf{x}$ and $\boldsymbol{\Theta}$ at time t_k given all previous observations, including $\mathbf{y}_k$. Furthermore, $p(\mathbf{y}_k)$ is the total probability of observation at time t_k which can be evaluated as follows:

$$p(\mathbf{y}_k) = \int \int p(\boldsymbol{\Theta}, \mathbf{x}|\mathbf{Y}_{k-1}) p(\mathbf{y}_k|\boldsymbol{\Theta}, \mathbf{x}) d\boldsymbol{\Theta} d\mathbf{x} \tag{20}$$

As discussed in the previous section, the PCQ approach provides us a tool to determine equations of evolutions for conditional moments for the prior joint pdf $p(\mathbf{\Theta}, \mathbf{x}|\mathbf{Y}_{k-1})$. We now seek to develop equations of evolutions for the posterior conditional moments. As a step towards this goal, let us consider a continuously differentiable scalar function $\phi(\mathbf{\Theta}, \mathbf{x})$ and define posterior and prior conditional moments as:

$$\hat{\phi}_k^+ = \mathbf{E}^+[\phi(\mathbf{\Theta}, \mathbf{x})] \triangleq \int\int \phi(\mathbf{\Theta}, \mathbf{x}) p(\mathbf{\Theta}, \mathbf{x}|\mathbf{Y}_k) d\mathbf{\Theta} d\mathbf{x} \tag{21}$$

$$\hat{\phi}_k^- = \mathbf{E}^-[\phi(\mathbf{\Theta}, \mathbf{x})] \triangleq \int\int \phi(\mathbf{\Theta}, \mathbf{x}) p(\mathbf{\Theta}, \mathbf{x}|\mathbf{Y}_{k-1}) d\mathbf{\Theta} d\mathbf{x} \tag{22}$$

Now, multiplying Eq. (19) with $\phi(\mathbf{\Theta}, \mathbf{x})$ and integrating over $\mathbf{\Theta}$ and $\mathbf{x}$, we get:

$$\hat{\phi}_k^+ = \frac{\mathbf{E}^-[\phi(\mathbf{\Theta}, \mathbf{x}) p(\mathbf{y}_k|\mathbf{\Theta}, \mathbf{x})]}{p(\mathbf{y}_k)} \tag{23}$$

Note that $\mathbf{y}_k$ is fixed with respect to the expectation operator and thus, the right-hand side of Eq. (23) is a function of $\mathbf{y}_k$ only. Notice that Eq. (23) is not an ordinary difference equation and the evaluation of right-hand side of Eq. (23) requires the knowledge of the prior density function. Although the PCQ process does not provide us a closed-form expression for the state or parameter pdf but it can be used effectively in computing the expectation integrals. As discussed in the previous section, all moments of random variables $\mathbf{\Theta}$ and $\mathbf{x}$ are just function of their PC expansion coefficients, i.e., $\mathbf{\Theta}_{pc}$ and $\mathbf{X}_{pc}$. Hence, one can just update the PC coefficients on the arrival of measurement data based upon Eq. (23). So if we define $\mathbf{\Theta}_{pc}^-$ and $\mathbf{X}_{pc}^-$ to be the prior PC coefficients and $\mathbf{\Theta}_{pc}^+$ and $\mathbf{X}_{pc}^+$ to be posterior PC coefficients, then we can evaluate $\hat{\phi}^-(\mathbf{\Theta}, \mathbf{x})$ and $\hat{\phi}^+(\mathbf{\Theta}, \mathbf{x})$ as:

$$\hat{\phi}_k^- = \mathbf{E}^-[\phi(\mathbf{\Theta}, \mathbf{x})] = \int \phi(\mathbf{\Theta}_{pc}^- \Phi(\boldsymbol{\xi}), \mathbf{X}_{pc}^-(t)\Phi(\boldsymbol{\xi})) p(\boldsymbol{\xi}) d\boldsymbol{\xi} \tag{24}$$

$$\hat{\phi}_k^+ = \mathbf{E}^+[\phi(\mathbf{\Theta}, \mathbf{x})] = \int \phi(\mathbf{\Theta}_{pc}^+ \Phi(\boldsymbol{\xi}), \mathbf{X}_{pc}^+(t)\Phi(\boldsymbol{\xi})) p(\boldsymbol{\xi}) d\boldsymbol{\xi} \tag{25}$$

Hence, prior and posterior mean for both state and parameter can be written as:

$$\hat{\mathbf{z}}_k^- \triangleq \mathbf{E}^-[\mathbf{z}_k] = \begin{bmatrix} \mathbf{X}_{pc_1}^-(t) \\ \mathbf{\Theta}_{pc_1}^- \end{bmatrix}, \ \mathbf{z}(t, \boldsymbol{\xi}) = \begin{bmatrix} \mathbf{x}(t, \boldsymbol{\xi}) \\ \mathbf{\Theta}(\boldsymbol{\xi}) \end{bmatrix} \tag{26}$$

$$\hat{\mathbf{z}}_k^+ \triangleq \mathbf{E}^+[\mathbf{z}_k] = \begin{bmatrix} \mathbf{X}_{pc_1}^+(t) \\ \mathbf{\Theta}_{pc_1}^+ \end{bmatrix} \tag{27}$$

Similarly, prior and posterior covariance matrices can be written as:

$$\mathbf{\Sigma}_k{}^- \triangleq \mathbf{E}^-[(\mathbf{z}_k - \hat{\mathbf{z}}_k^-)(\mathbf{z}_k - \hat{\mathbf{z}}_k^-)^T] = \begin{pmatrix} \sum_{i=1}^N \mathbf{X}_{pc_i}^{-2} & \sum_{i=1}^N \mathbf{X}_{pc_i}^- \mathbf{\Theta}_{pc_i}^- \\ \sum_{i=1}^N \mathbf{X}_{pc_i}^- \mathbf{\Theta}_{pc_i}^- & \sum_{i=1}^N \mathbf{\Theta}_{pc_i}^{-2} \end{pmatrix} \tag{28}$$

$$\mathbf{\Sigma}_k^+ \triangleq \mathbf{E}^+[(\mathbf{z}_k - \hat{\mathbf{z}}_k^-)(\mathbf{z}_k - \hat{\mathbf{z}}_k^-)^T] = \begin{pmatrix} \sum_{i=1}^N \mathbf{X}_{pc_i}^{+2} & \sum_{i=1}^N \mathbf{X}_{pc_i}^+ \mathbf{\Theta}_{pc_i}^+ \\ \sum_{i=1}^N \mathbf{X}_{pc_i}^+ \mathbf{\Theta}_{pc_i}^+ & \sum_{i=1}^N \mathbf{\Theta}_{pc_i}^{+2} \end{pmatrix} \tag{29}$$

where, $\mathbf{X}_{pc_i}^-$ and $\mathbf{\Theta}_{pc_i}^-$ are the i^{th} column of the PC expansion coefficient matrices $\mathbf{X}_{pc}^-$ and $\mathbf{\Theta}_{pc}^-$, respectively. Similarly, $\mathbf{X}_{pc_i}^+$ and $\mathbf{\Theta}_{pc_i}^+$ are the i^{th} column of unknown PC expansion coefficient matrices $\mathbf{X}_{pc}^+$ and $\mathbf{\Theta}_{pc}^+$, respectively. According to the minimum variance formulation, the posterior mean and covariance can be computed given an estimate of prior mean and covariance [36]:

$$\hat{\mathbf{z}}_k^+ = \hat{\mathbf{z}}_k^- + \mathbf{K}_k[\tilde{\mathbf{y}}_k - \mathbf{E}^-[\mathbf{h}(\mathbf{x}_k)]] \tag{30}$$

$$\mathbf{\Sigma}_k^+ = \mathbf{\Sigma}_k^- + \mathbf{K}_k \mathbf{\Sigma}_{zy} \tag{31}$$

$$\mathbf{K}_k = -\mathbf{\Sigma}_{zy}^T \left(\mathbf{P}_{hh}^- + \mathbf{R}_k\right)^{-1} \tag{32}$$

It should be noted that the minimum variance formulation is valid for any pdf although it makes use of only mean and covariance information. $\tilde{\mathbf{y}}_k$ denotes the sensor output at time t_k while function $\mathbf{h}(\mathbf{x}, \boldsymbol{\Theta})$ provides a true model between sensor output $\mathbf{y}$ and states, $\mathbf{x}$. $\mathbf{R}_k$ denotes the measurement noise error covariance matrix. $\mathbf{K}_k$ is known as the Kalman gain matrix and matrices $\boldsymbol{\Sigma}_{zy}$ and $\boldsymbol{\Sigma}_{zz}$ are defined as:

$$\hat{\mathbf{h}}_k^- \triangleq \mathbf{E}^-[\mathbf{h}(\mathbf{x}_k, \boldsymbol{\Theta})] = \sum_{q=1}^{M} w_q \underbrace{\mathbf{h}(\mathbf{x}_k(\boldsymbol{\xi}_q))}_{\mathbf{h}_q}, \; \boldsymbol{\Sigma}_{zy} \triangleq \mathbf{E}^-[(\mathbf{z}_k - \hat{\mathbf{z}}_k)(\mathbf{h}(\mathbf{x}_k) - \hat{\mathbf{h}}_k^-)^T] = \sum_{q=1}^{M} w_q(\mathbf{z}_k(\boldsymbol{\xi}_q) - \hat{\mathbf{z}}_k^-)(\mathbf{h}_q - \hat{\mathbf{h}}_k^-)^T \tag{33}$$

$$\boldsymbol{\Sigma}_{hh}^- \triangleq \mathbf{E}^-[(\mathbf{h}(\mathbf{x}_k) - \hat{\mathbf{h}}_k^-)(\mathbf{h}(\mathbf{x}_k) - \hat{\mathbf{h}}_k^-)^T] = \sum_{q=1}^{M} w_q(\mathbf{h}_q - \hat{\mathbf{h}}_k^-)(\mathbf{h}_q - \hat{\mathbf{h}}_k^-)^T \tag{34}$$

Notice that Eq. (27) and Eq. (30) provide a closed-form solution for $\mathbf{X}_{pc_1^+}$ and $\boldsymbol{\Theta}_{pc_1}^+$ while one can solve for rest of the posterior coefficients while making use of Eq. (29) and Eq. (31).

5. Numerical Experiments

For validation purposes, we consider the Eyjafjallajökulleruption scenario. The `puff` Lagrangian VATD model was used to propagate ash parcels in a given wind field (NCEP Reanalysis) [22] through time concentrating on the period 14–16 April 2010. `puff` takes into account dry deposition by particle fallout, as well as dispersion and advection.Variability in the height and loading of the eruption is introduced through the volcano column model `bent`. Table 1 lists all source variables together with their assumed uncertainties. Output uncertainty due to uncertain input parameters is determined with a polynomial chaos quadrature-based sampling of the multidimensional puff input vector space. Following runs of `bent` at the quadrature points, each `bent` output is then propagated through `puff`, which was then run for a real-time period of two days. The outputs from `puff` were then combined to produce the ensemble by applying the appropriate weight to each deterministic `bent`–`puff` run. For simulation purposes, a random sample of source variable is used to create an artificial satellite imagery depicting ash top-height. The satellite imagery data is assumed to be available every 6 hours during the two day simulation period.

Table 1: Eruption source parameters based on observations of Eyjafjallajökull volcano and information from other similar eruptions of the past.

Parameter	Value range	PDF	Comment
Vent radius, b_0, m)	65-150	Uniform, + definite	Measured from IMO radar image of summit vents on 14 April 2010
Vent velocity, w_0, m/s)	Range: 45-124	Uniform, + definite	Measured by infrasound [37] 6-21 May, when MER similar to 14-18 April
Mean grain size, Md_φ, φ units	2 boxcars: 1.5-2 and 3-5	Uniform, $\in \mathbb{R}$	[38], Table 1, vulcanian and phreatoplinian. A. Hoskuldsson, Eyjafjallajökull Eruption Workshop, 09/2010, presentation, quote: 'vulcanian with unusual production of fine ash'.
σ_φ, φ units	2.0 – 6	Uniform, $\in \mathbb{R}$	[38], Table 1, vulcanian and phreatoplinian

For this set of simulations we compared the simulation outputs for 9^4 and 13^4 samples (quadrature points) and the results indicate that 9^4 runs yields substantially the same results for mean and variance for ash top-height as 13^4 runs. Similarly, the comparison of using 10^5 to 10^7 particles in the `puff` simulation also indicated that the choice of 4×10^6 particles was adequate for our purposes, and consistent with the findings of others [39].

Fig. 1 shows probability of ash being present at a given geological location along with synthetic satellite observed ash top-height data for 16^{th} April, 2010. As expected, the PCQ generated ash cloud footprint is quite large due to large uncertainty in prior source parameters. It should be noticed that most of the satellite data lies with in high probability region. We mention that 4^{th} order PC expansion is used to computed these probability contours as discussed in Ref. [33]. Fig. 2 show the estimated source parameters along with 3σ bounds while making use of the PCQ based minimum variance estimator as discussed in Section 4. The solid red line represents the assumed true value for source parameters while green squares corresponds to estimated source parameters. Furthermore, blue asterisks represent $\pm 3\sigma$ bounds. From these figures, it is clear that the uncertainty associated with source parameters decreases as the number of observations increases. These preliminary results clearly illustrates the effectiveness of proposed ideas in estimating the posterior distribution for source parameters.

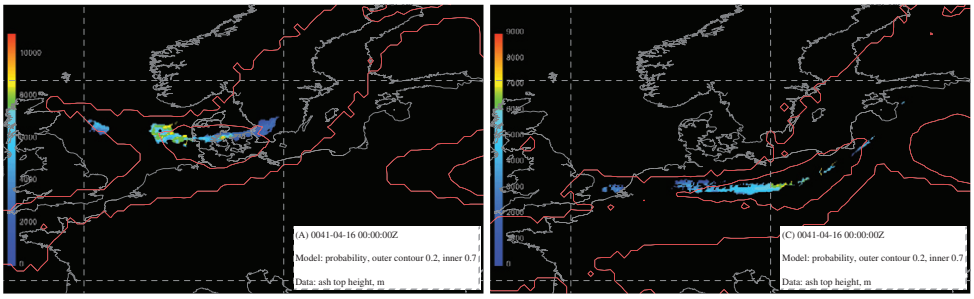

(a) April 16^{th}, 0000 hrs (b) April 16^{th}, 1200 hrs

Figure 1: Probability Contours and Satellite Image

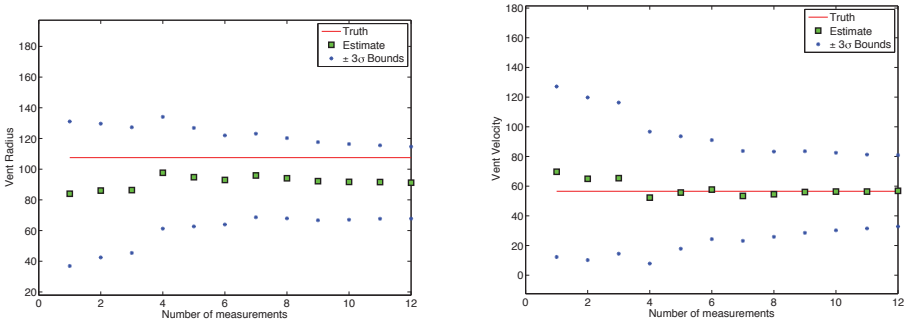

(a) Vent Radius (b) Vent Velocity

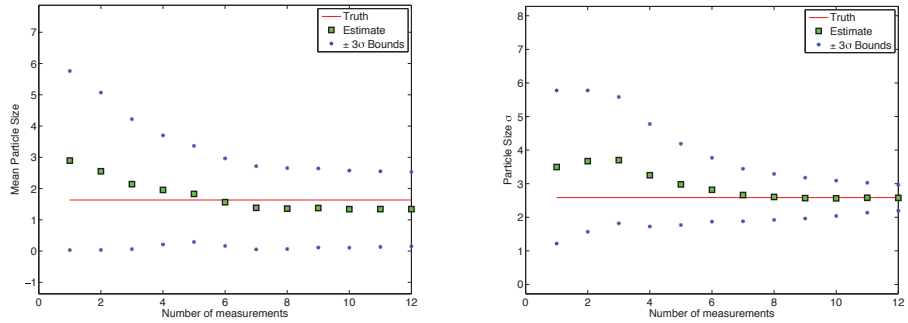

(c) Mean Particle Size (d) Particle Size Sigma

Figure 2: Estimated Source Parameters

6. Acknowledgement

This material is based upon work supported by the National Science Foundation under Awards No. CMMI-1054759 and CMMI-1131074.

References

[1] D. Schneider, W. Rose, L. Kelley, Tracking of 1992 eruption clouds from Crater Peak vent of Mount Spurr Volcano, Alaska using AVHRR, U. S. Geological Survey Bulletin 2139 (1995) 27–36.
[2] CNN, New ash cloud could extend air travel threat, Accessed at http://www.cnn.com/2010/TRAVEL/04/19/volcano.ash/index.html.

[3] D. B. Ryall, R. H. Maryon, Validation of the uk met. offices name model against the etex dataset, Atmospheric Environment 32 (1998) 4265–4276.
[4] A. Jones, Assessing the meteorological uncertainties in dispersion forecasts using nwp ensemble prediction systems, in: Proceedings of the 11th International Conference on Harmonisation within Atmospheric Dispersion Modelling for Regulatory Purposes, Cambridge, England, UK, 2007, pp. 246–250, http://www.harmo.org/Conferences/Proceedings/_Cambridge/publishedSections/Op246-250.pdf.
[5] R. E. Kalman, A New Approach to Linear Filtering and Prediction Problems 1, Transactions of the ASME–Journal of Basic Engineering 82 (Series D) (1960) 35–45.
[6] A. H. Jazwinski, Stochastic Processes and Filtering Theory, Academic Press, 1970.
[7] S. F. Schmidt, Application of State-Space Methods to Navigation Problems, Advanced Control Systems 3 (1966) 293–340.
[8] B. D. O. Anderson, J. B. Moore, Optimal Filtering, Prentice-Hall, 1979, 277-297.
[9] S. J. Julier, New extension of the Kalman filter to nonlinear systems, Proceedings of SPIE (1997) 182–193doi:10.1117/12.280797.
URL http://link.aip.org/link/?PSI/3068/182/1&Agg=doi
[10] F. E. Daum, Bounds on performance for multiple target tracking, Automatic Control, IEEE Transactions on 35 (4) (1990) 443–446. doi:10.1109/9.52299.
[11] F. Daum, S.-T. Yau, S. Yau, Comments on "finite-dimensional filters with nonlinear drift" [and addendum], Aerospace and Electronic Systems, IEEE Transactions on 34 (2) (1998) 689–692. doi:10.1109/7.670361.
[12] I. H. Sloan, H. Woniakowski, When are quasi-monte carlo algorithms efficient for high dimensional integrals?, Journal of Complexity (1998) 1–33.
[13] Special issue on monte carlo methods for statstical signal processing, IEEE Trasactions on Signal Processing 50 (2).
[14] F. Daum, J. Huang, Curse of dimensionality and particle filters, Aerospace Conference, 2003. Proceedings. 2003 IEEE 4 (March 8-15, 2003) 1979–1993.
[15] J. Li, D. Xiu, A generalized polynomial chaos based ensemble Kalman filter with high accuracy, Journal of Computational Physics 228 (15) (2009) 5454–5469. doi:10.1016/j.jcp.2009.04.029.
URL http://linkinghub.elsevier.com/retrieve/pii/S0021999109002137
[16] B. L. Pence, H. K. Fathy, J. L. Stein, A Maximum Likelihood Approach To Recursive Polynomial Chaos Parameter Estimation, in: 2010 American Control Conference, Marriott Waterfront, Baltimore, MD, USA, 2010, pp. 2144–2151.
[17] E. Blanchard, A Polynomial-chaos based Bayesian approach for estimating uncertain parametersof mechanical systems, in: Proceedings of the ASME 2007 International Design Engineering Technical Conferences & Computers and Information in Engineering Conference IDETC/CIE 2007, 2007, pp. 1–9.
[18] R. Madankan, Polynomial Chaos Based Method for State and Parameter Estimation, Ph.D. thesis, State University of New York at Buffalo (2011).
[19] S. Carey, R. Sparks, Quantitative models of the fallout and dispersal of tephra from volcanic eruption columns, Bull. Volcanology 48 (1986) 109–125.
[20] T. Suzuki, A theoretical model for dispersion of tephra, Terra Scientific Publishing, Tokyo, 2005, pp. 95–116.
[21] H. Tanaka, Development of a prediction scheme for the volcanic ash fall from redoubt volcano, in: First Int'l Symposium on Volcanic Ash and Aviation Safety, Seattle, 1991, p. 58.
[22] C. Searcy, K. Dean, B. Stringer, PUFF: A volcanic ash tracking and prediction model, J. Volcanology and Geophysical Research 80 (1998) 1–16.
[23] P. Webley, K. Dean, J. Dehn, J. Bailey, R. Peterson, Volcanic ash dispersion modeling of the 2006 eruption of Augustine Volcano , USGS Professional Paper: Augustine Volcano 2006 eruption.
[24] R. S. J. Sparks, M. I. Bursik, S. N. Carey, J. S. Gilbert, L. S. Glaze, H. Sigurdsson, A. W. Woods, Volcanic Plumes, John Wiley & Sons, London, 1997, 574p.
[25] M. Bursik, S. Kobs, A. Burns, O. Braitseva, L. Bazanova, I. Melekestsev, A. Kurbatov, D. Pieri, Volcanic plumes and the wind: jetstream interaction examples and implications for air traffic, J. of Volcanology and Geothermal Research 186 (2009) 60–67.
[26] M. Bursik, Effect of wind on the rise height of volcanic plumes, Geophys. Res. Lett. 18 (2001) 3621–3624.
[27] B. Morton, J. Turner, G. Taylor, Gravitational turbulent convection from maintained and instantaneous sources, Proceedings Royal Soc. London Ser. A 234 (1956) 1–23.
[28] A. Doucet, N. de Freitas, N. Gordon, Sequential Monte-Carlo Methods in Practice, Springer-Verlag, 2001, 6-14.
[29] R. N. Iyengar, P. K. Dash, Study of the random vibration of nonlinear systems by the gaussian closure technique, Journal of Applied Mechanics 45 (1978) 393–399.
[30] J. B. Roberts, P. D. Spanos, Random Vibration and Statistical Linearization, Wiley, 1990, 122-176.
[31] D. Xiu, G. Karniadakis, The wiener-askey polynomial chaos for stochastic differential equations, SIAM J. Scientific Computation 24 (2002) 619–644.
[32] N. Wiener, The Homogeneous Chaos, American Journal of Mathematics 60 (4) (1938) 897–936.
[33] K. Dalbey, A. Patra, E. Pitman, M. Bursik, M. Sheridan, Input uncertainty propagation methods and hazard mapping of geophysical mass flows, J. of Geophysical Research 113 (2008) B05203.
[34] E. W. Cheney, D. Kincaid, Numerical Mathematics and Computing, Brooks/Cole, Pacific Grove, CA, 1999.
[35] C. W. Clenshaw, A. R. Curtis, A method for numerical integration on an automatic computer, Numerische Mathematik 2 (1960) 197–205.
[36] A. Gelb, Applied Optimal Estimation, MIT Press, 1974.
[37] M. Ripepe, S. D. Angelis, G. Lacanna, B. Voight, Observation of infrasonic and gravity waves at soufriere hills volcano, montserrat, Geophysical Research Letters 37 (2010) L00E14, doi:10.1029/2010GL042557.
[38] A. W. Woods, M. I. Bursik, Particle fallout, thermal disequilibrium and volcanic plumes, Bulletin of Volcanology 53 (1991) 559–570.
[39] S. Scollo, M. Prestilippo, M. Coltelli, R. Peterson, G. Spata, A statistical approach to evaluate the tephra deposit and ash concentration from PUFF model forecasts, Journal of Volcanology and Geothermal Research 200 (2011) 129–142.